

Supporting information

Selectivity of Terpyridine platinum anti-cancer drugs for G-quadruplex DNA

**Elodie Morel^{1,2,†}, Claire Beauvineau^{1,2,†}, Delphine Naud-Martin^{1,2}, Corinne Landras-Guetta^{1,2},
Daniela Verga^{1,2}, Deepanjan Ghosh^{1,2}, Sylvain Achelle^{1,2,3}, Florence Mahuteau-Betzer^{1,2}, Sophie
Bombard^{1,2,*} and Marie-Paule Teulade-Fichou^{1,2*}**

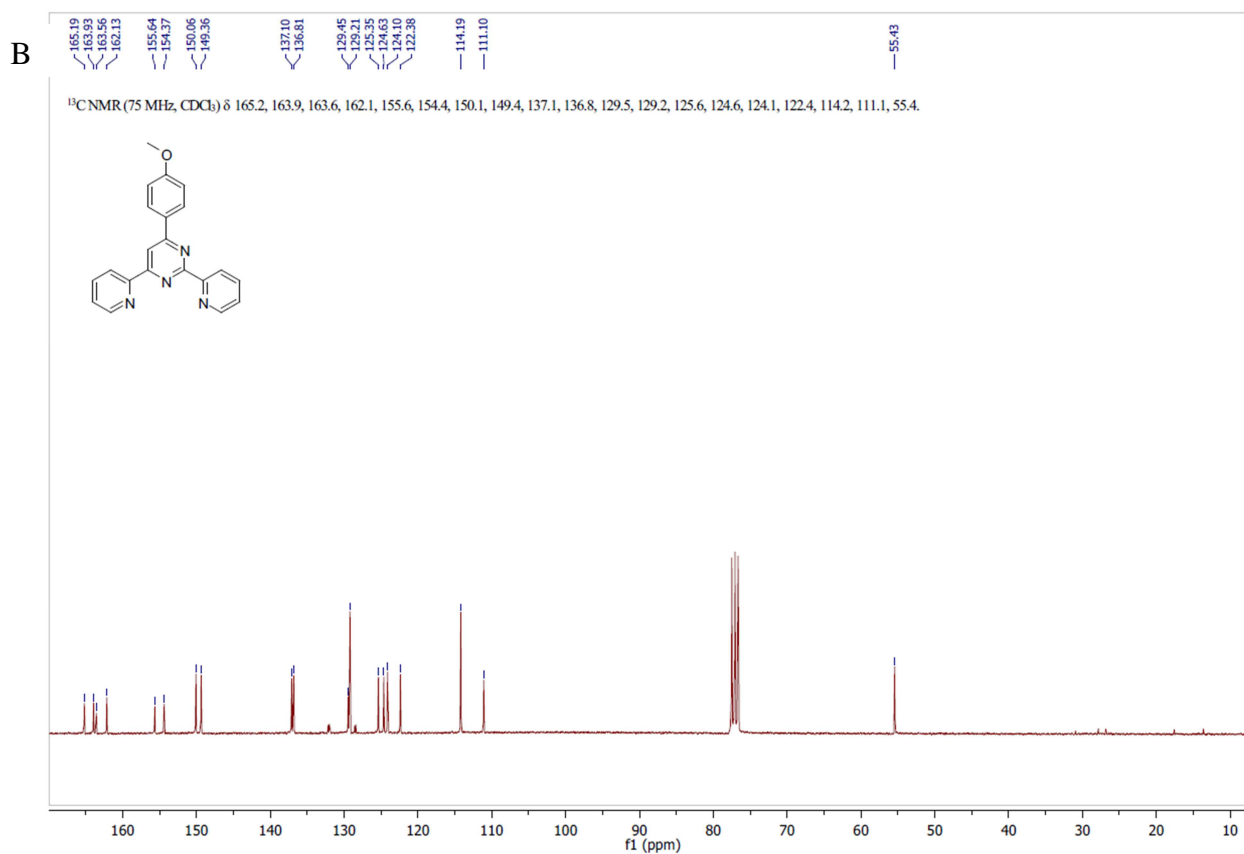
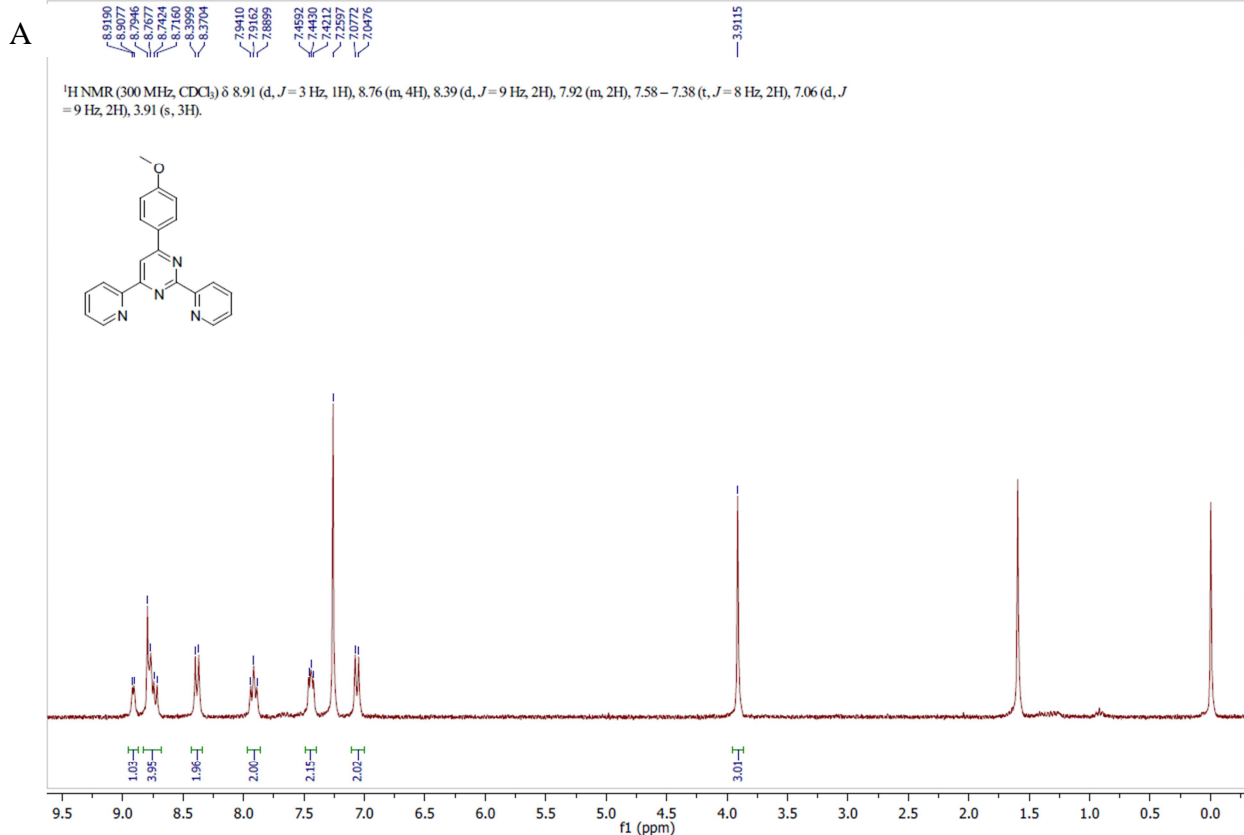
¹ Institut Curie, PSL Research University, CNRS-UMR 9187, INSERM U1196, F-91405, Orsay, France.

² Université Paris Sud, Université Paris-Saclay, CNRS-UMR 9187, INSERM U1196, F-91405 Orsay, France

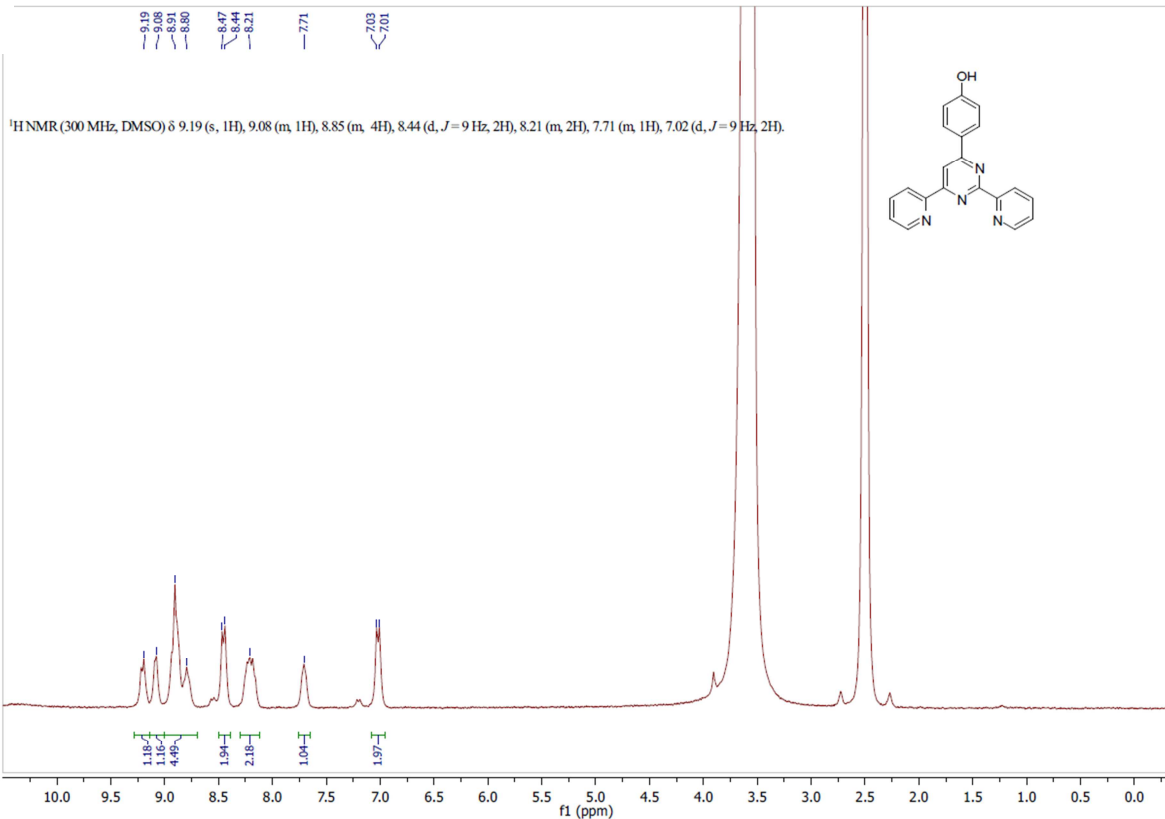
³ Univ Rennes, CNRS, ISCR-UMR 6226, F-35000 Rennes, France

* Correspondence marie-paule.teulade-fichou@curie.fr (M-P.T-F) and sophie.bombard@curie.fr (S.B); Tel.: 33169863086 and 33169863189

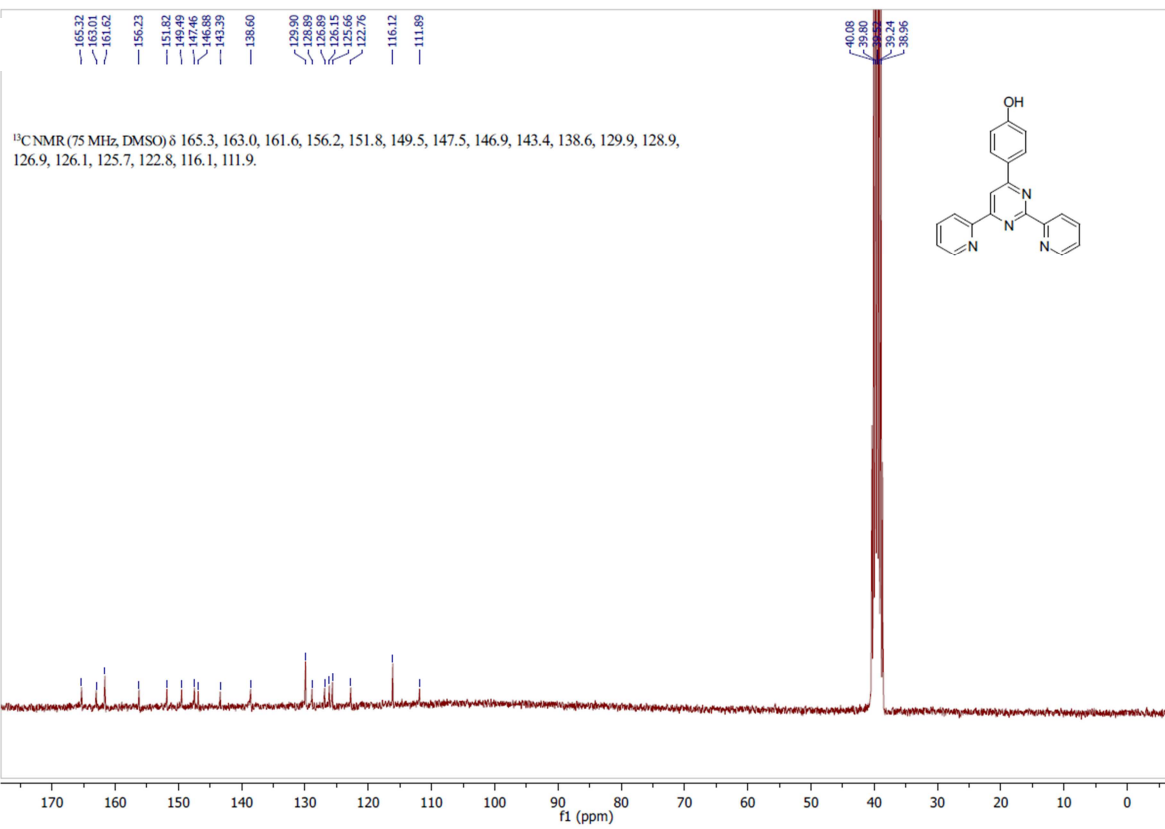
† These authors contributed equally to this work.



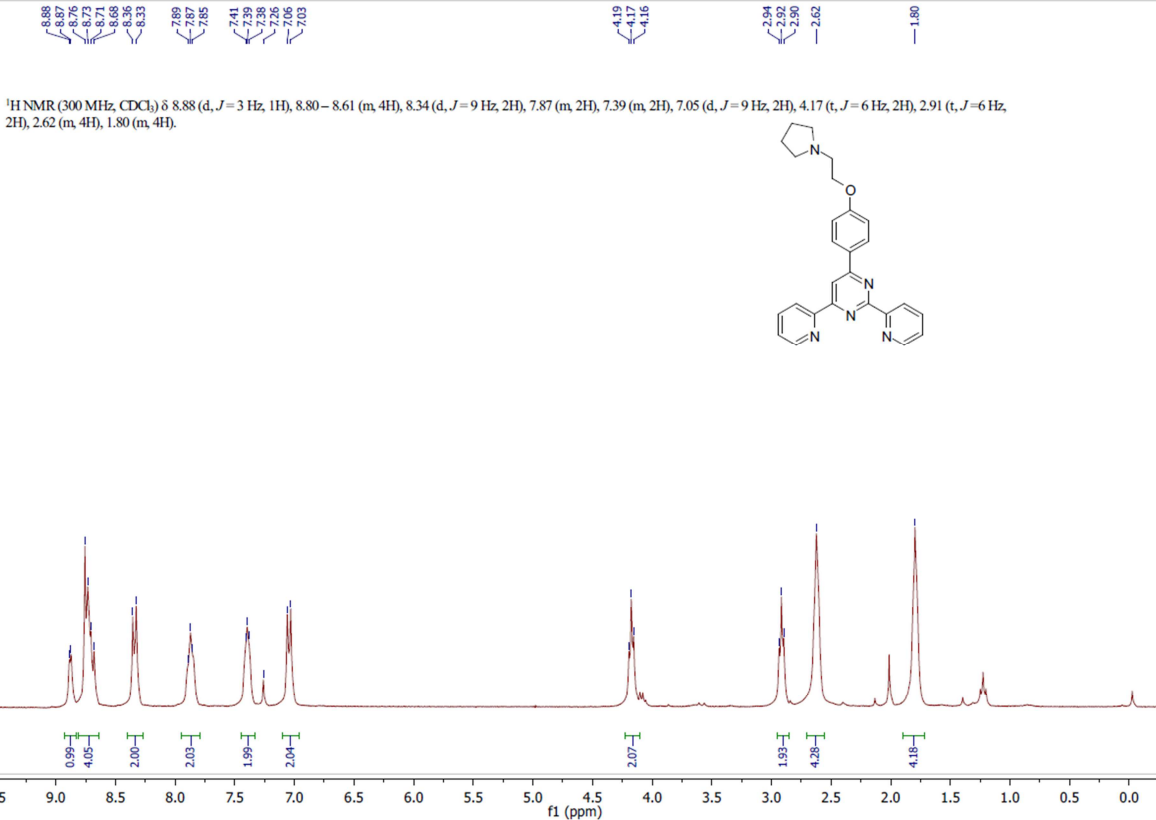
C



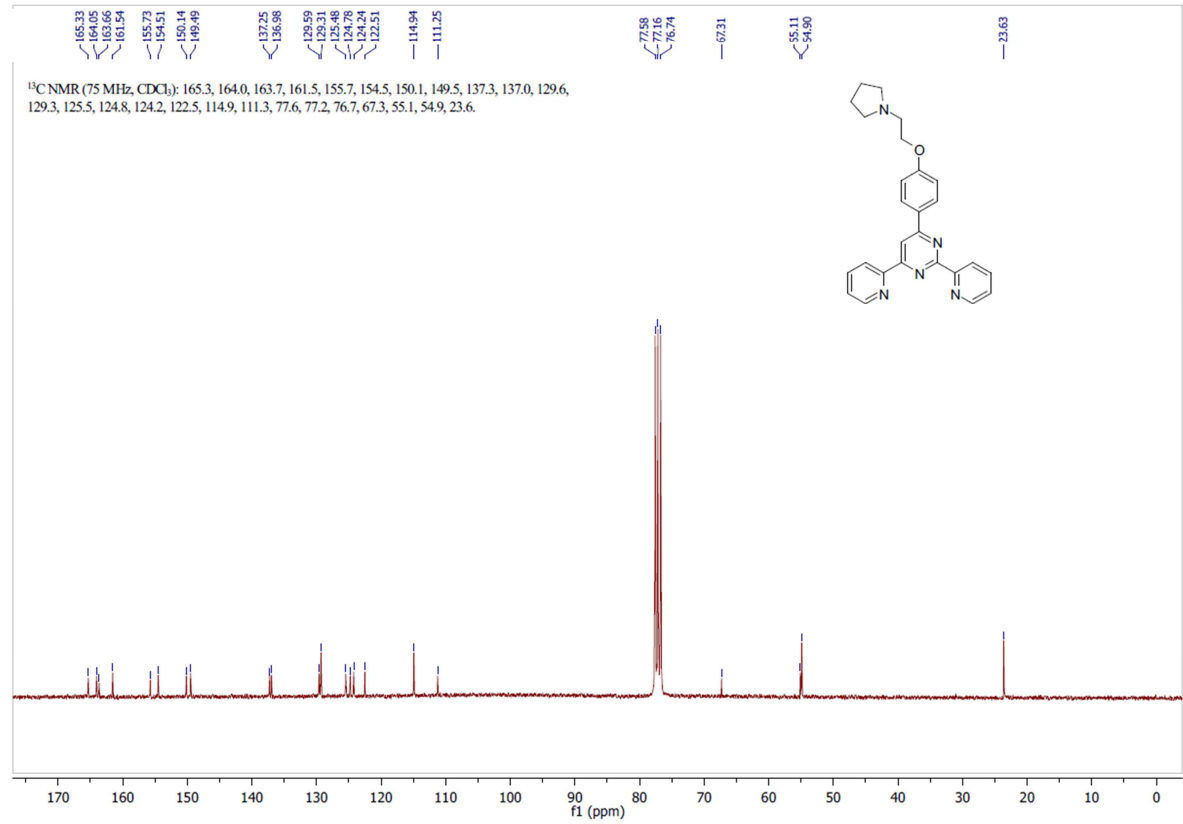
D



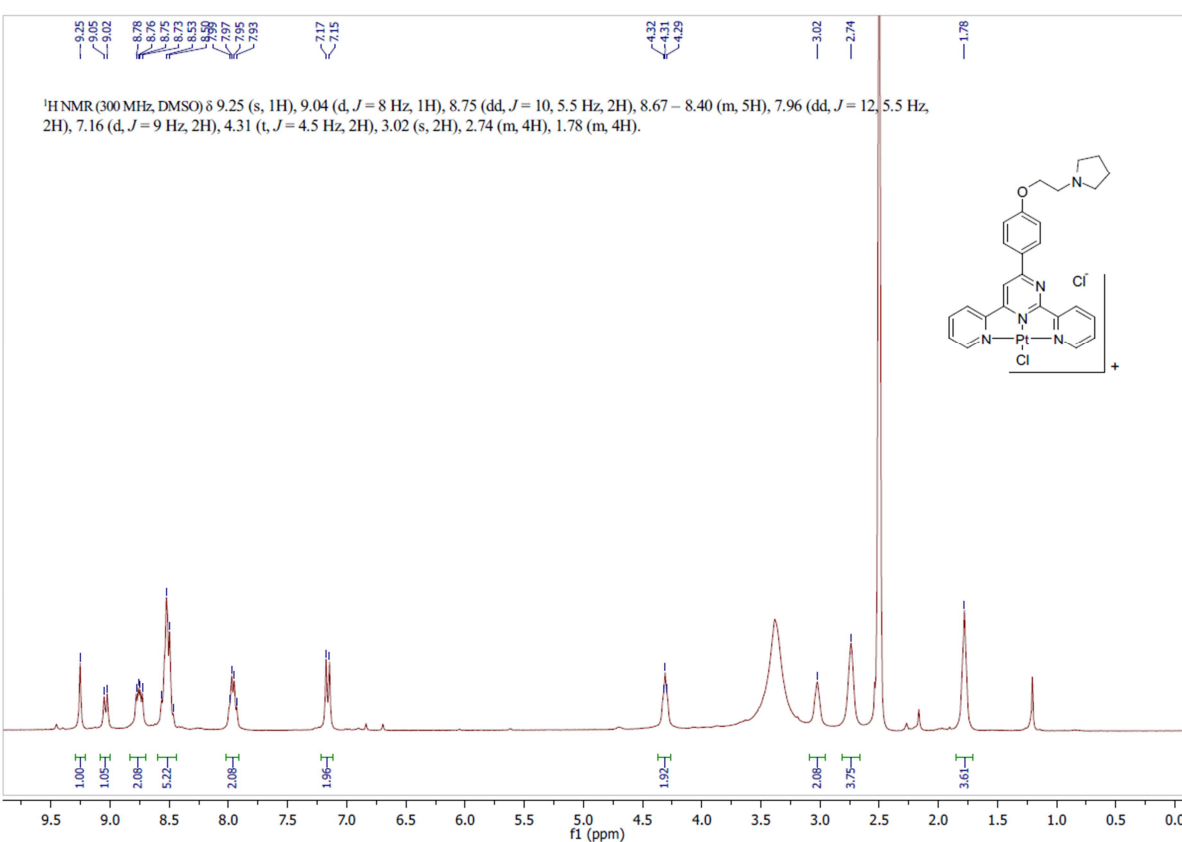
E



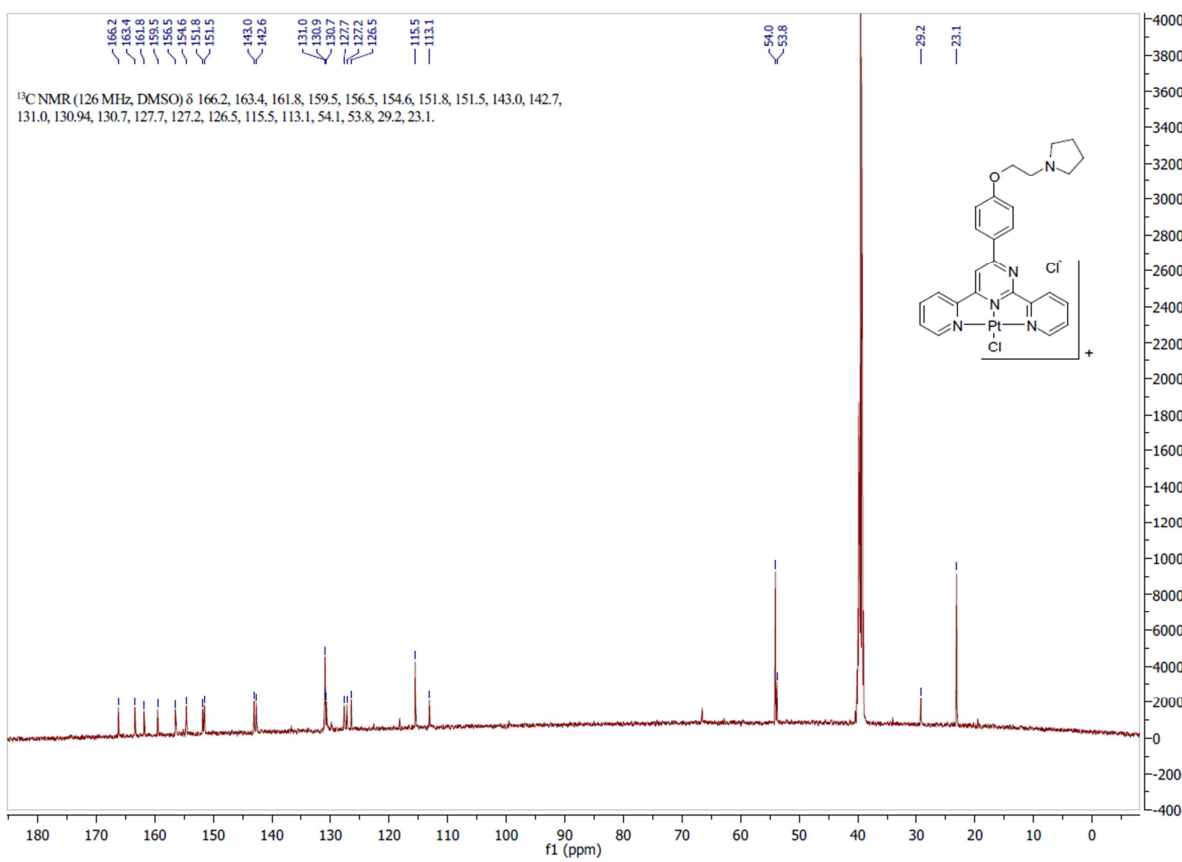
F

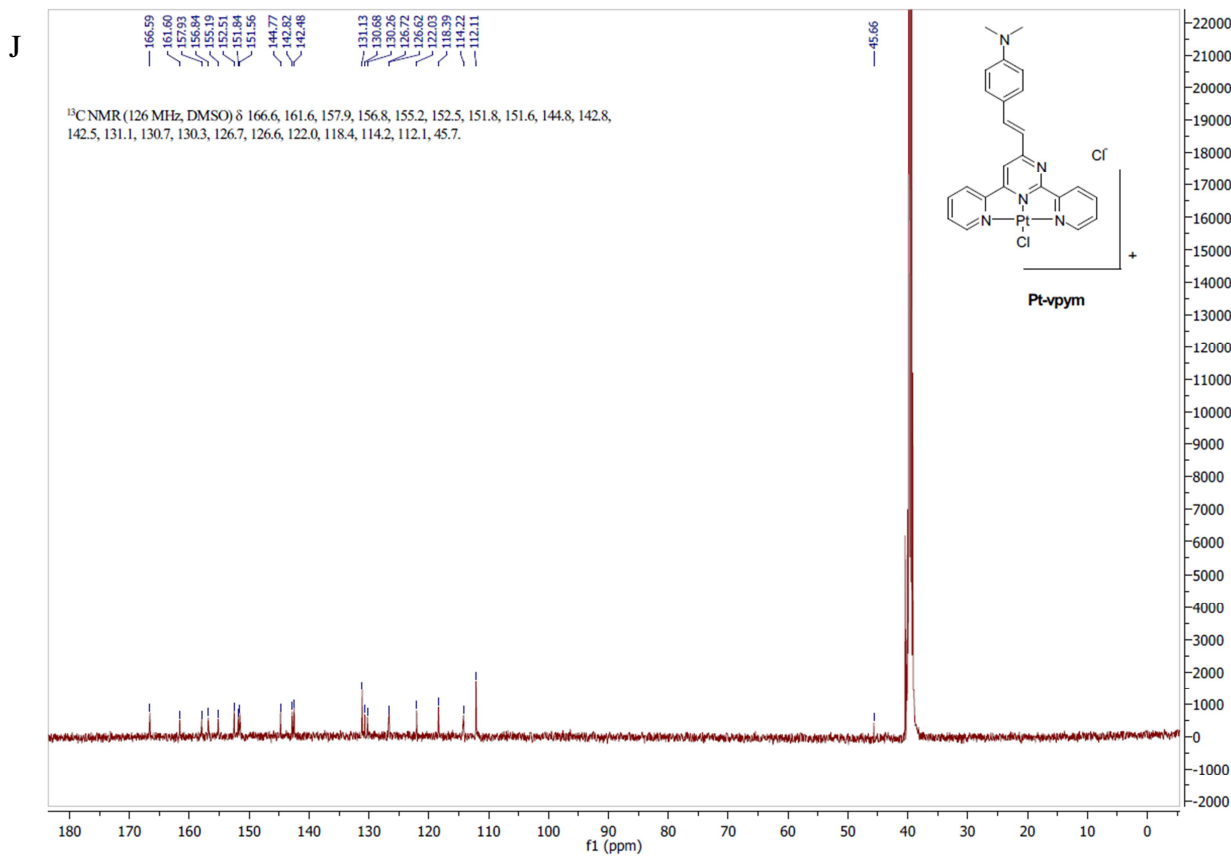
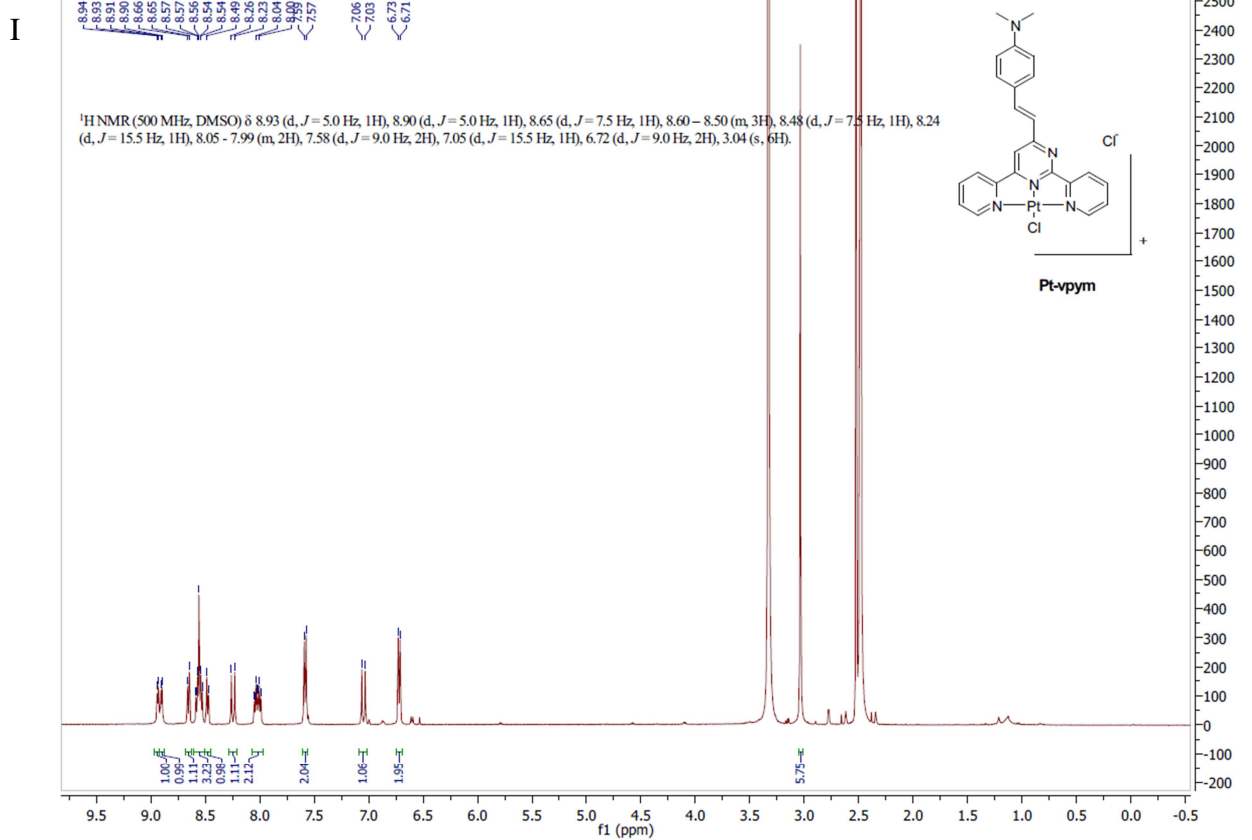


G



H





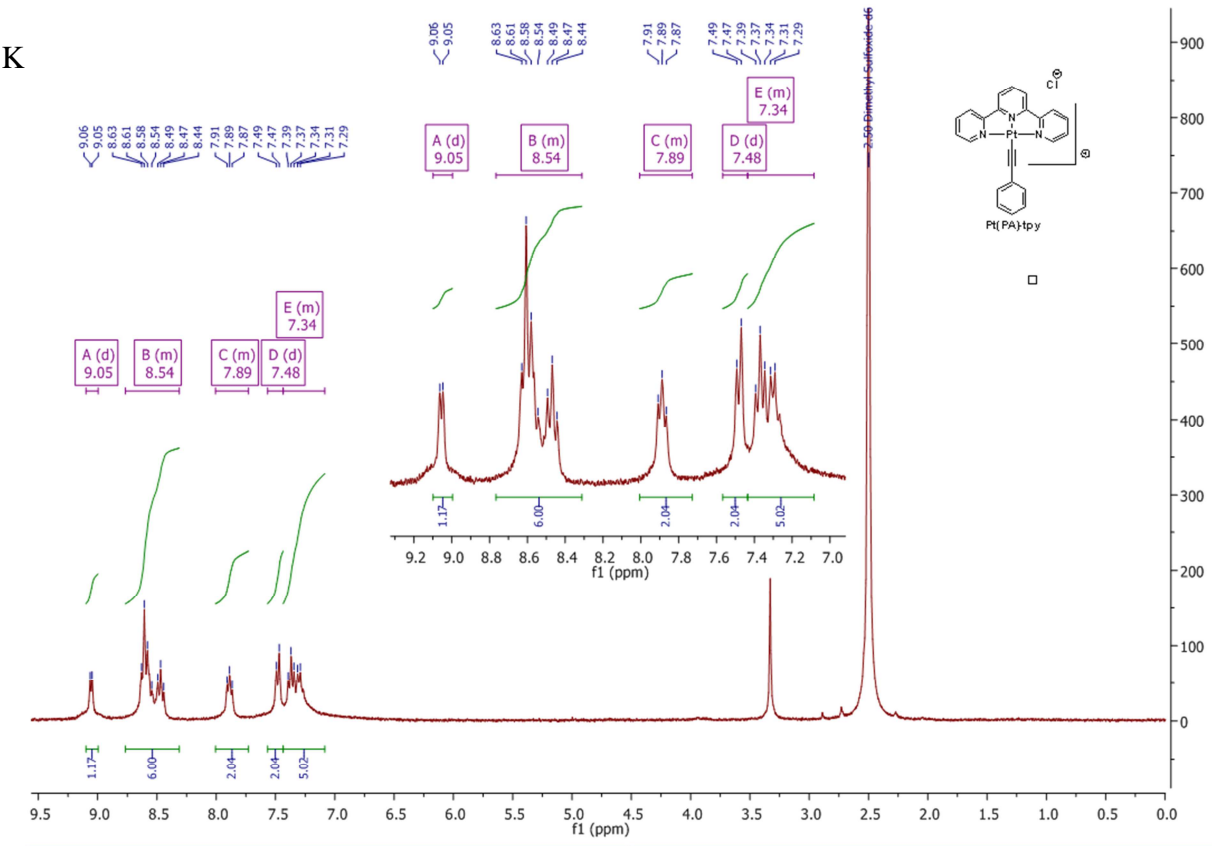


Figure S1: ^1H NMR and ^{13}C spectra, respectively, of compound **2** (A, B), compound **3** (C, D), **c pym** (E, F), **Pt-c pym** (G, H), **Pt-v pym** (I, J) and ^1H NMR spectrum of **Pt(PA)-tpy** (K).

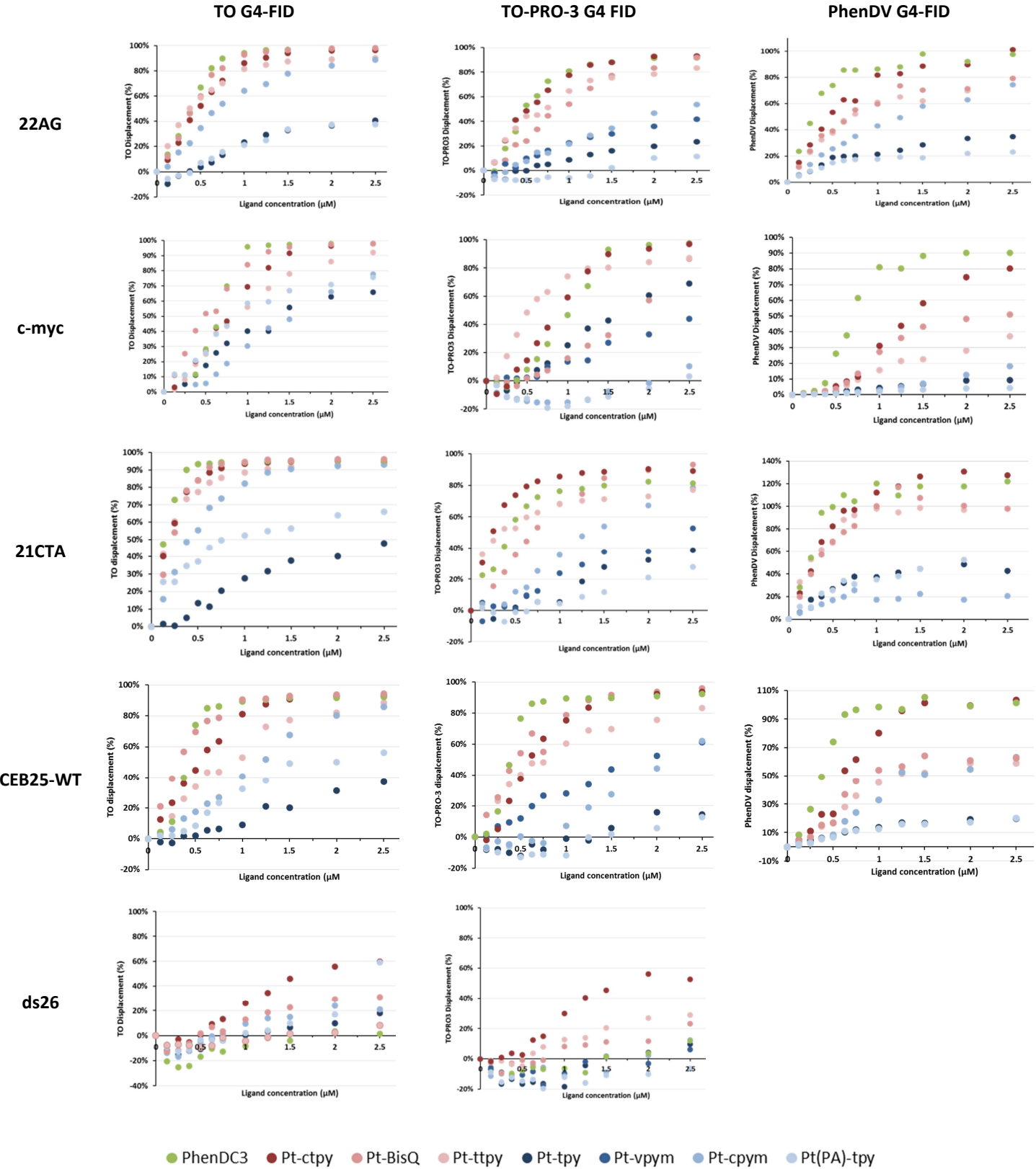


Figure S2. Fluorescence Intercalator Displacement (FID) assays, for compounds **Pt-BisQ**, **Pt-ctpy**, **Pt-ttpp**, **Pt-cpym**, **Pt-vpym**, **Pt(PA)-tpy** and **Pt-tpy** with G4 DNA (22AG, c-myc, 21CTA and 25CEBWT, 0,25 μ M) in presence of Thiazole Orange (TO), TO-PRO-3 (2 equivalents), and PhenDV (1.5 equivalents). Affinities of ligands are expressed by probe displacement as indicated in material and methods. Buffer used is K⁺100 (10 mM lithium cacodylate, 100 mM KCl and 1 % DMSO, pH = 7.3).

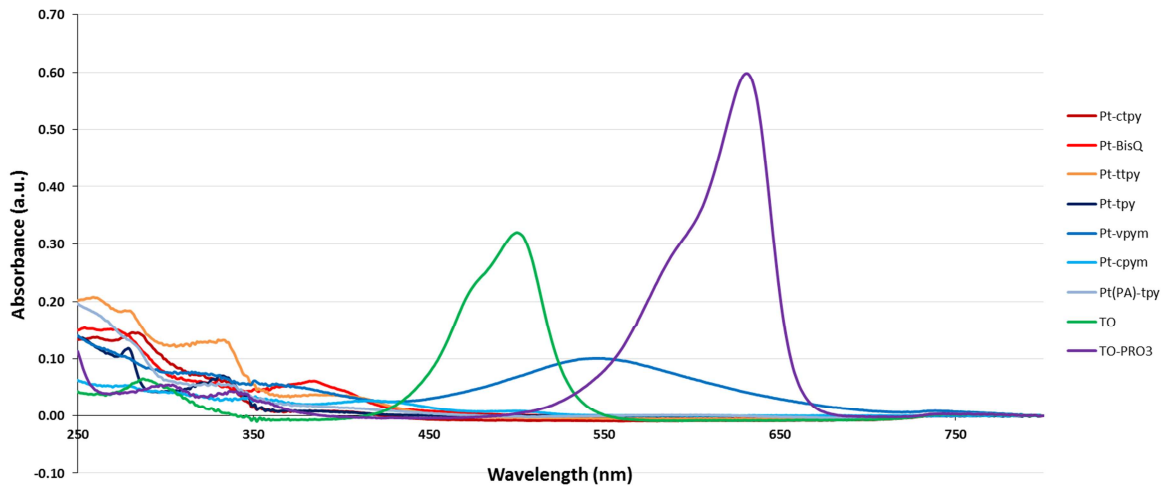


Figure S3. UV-Vis spectra of Pt-complexes, TO and TO-PRO-3 at 5 μ M in water.

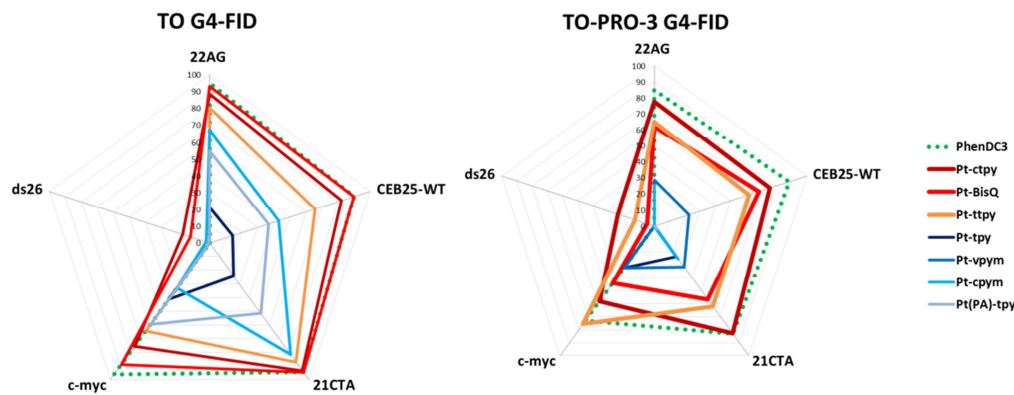


Figure S4: % of probe displacement at 1 μ M ligand (Pt-BisQ, Pt-ctpy, Pt-ttpy, Pt-cpym, Pt-vpym, Pt(PA)-tpy and Pt-tpy and PhenDC3 used as control) from G4-FID assay. Experiments are performed on the G-quadruplex structure of 22AG, c-myc, 21CTA, CEB25WT (as shown in Figure 1A) and on duplex ds26 DNA (0,25 μ M), with thiazole orange (TO) (2 eq. for G4-DNA & 3eq. for ds26), TO-PRO-3 (2 eq. for G4-DNA & 3eq. for ds26) in K⁺100 buffer (100 mM KCl and 10 mM lithium cacodylate, pH = 7.3).

PLATINATION OF G-QUADRUPLEX DNA

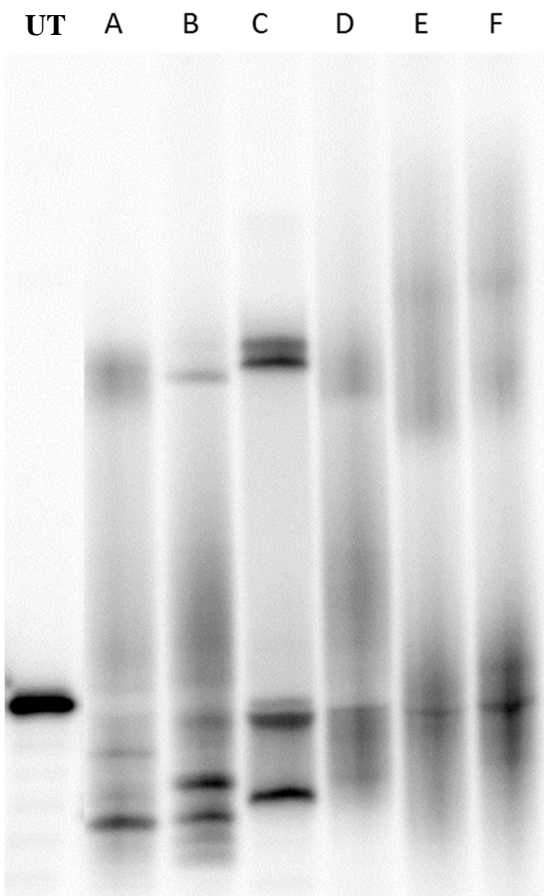


Figure S5. Denaturing gel electrophoresis (15 % acrylamide) of platination reactions induced by 2 equivalents of compounds **Pt-ttptpy** (A), **Pt-tpy** (B), Pt-BisQ (C), **Pt-ctpy** (D), **Pt-cpym** (E), and **Pt-vpym** (F) on c-myc (100 μ M) in the presence of K⁺100 buffer after 18h incubation at 32°C. Lane labelled with UT corresponds to untreated c-myc.

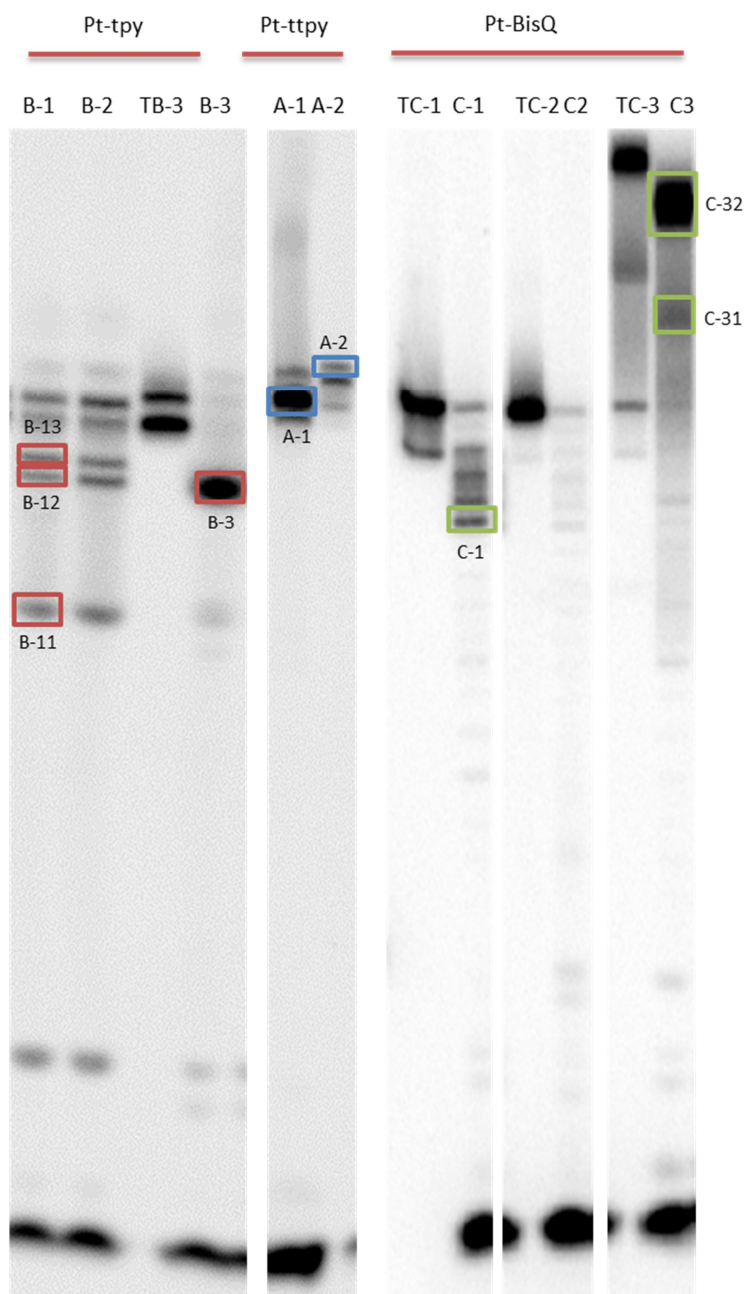


Figure S6. Denaturing gel electrophoresis (20% acrylamide) of 3'-exonuclease digestion of bands obtained by platination of c-myc with **Pt-tpy**, **Pt-tppy** and **Pt-BisQ** from Figure 4. Lane labelled with T corresponds to the non-digested bands.

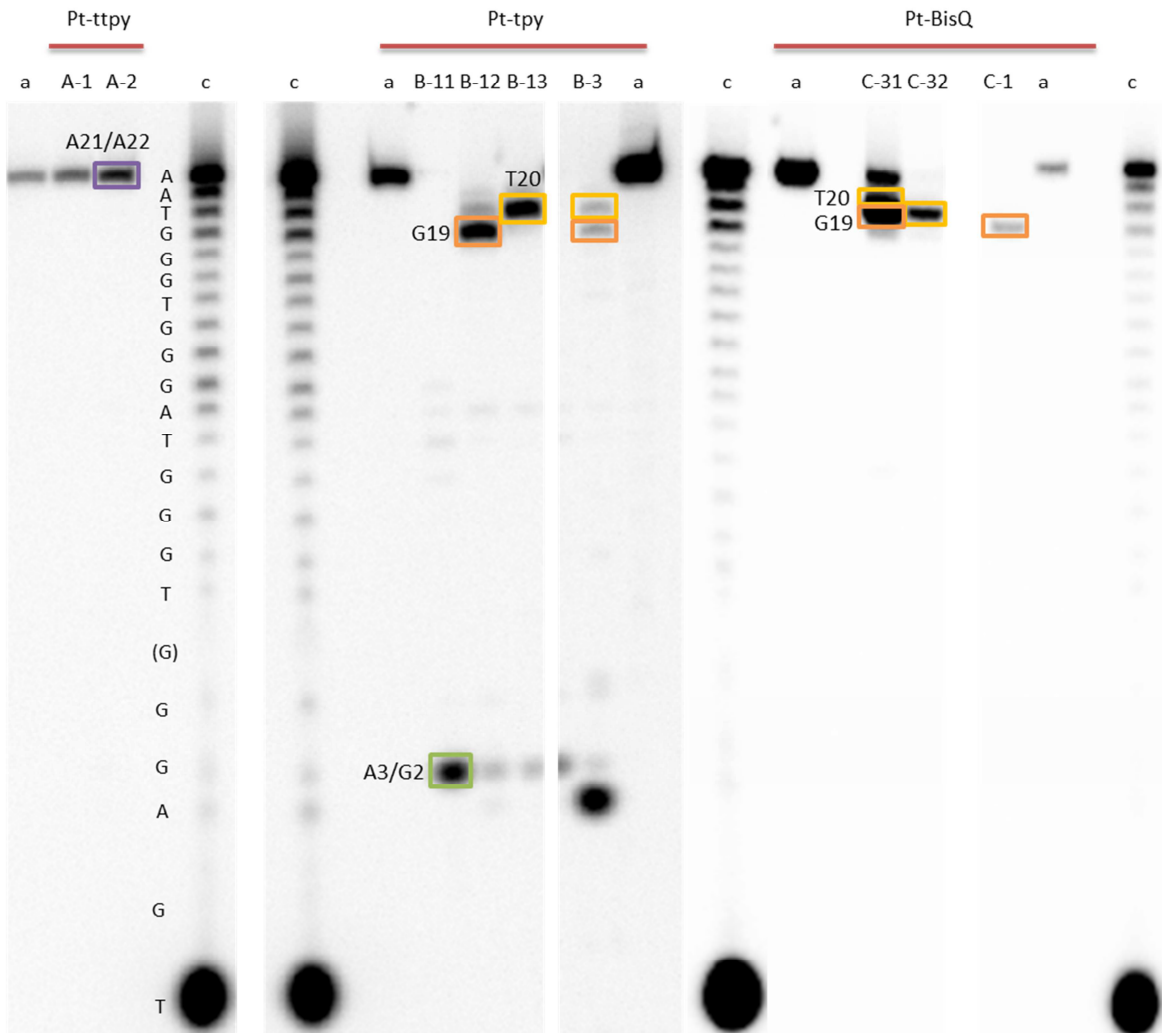


Figure S7. Denaturing gel electrophoresis (20% acrylamide) of the fragments of digestion from Figure S6 after deplatination using NaCN 0.2M at 32 °C for 18 hours. Lane c corresponds to the partial digestion of non-platinated DNA c-myc (0.008 unit enzyme/ μ M), and it gives the reference scale for the migration of the deplatinated digested fragments. Lane a corresponds to the non-digested oligonucleotide c-myc. The letter and number indicate the platinum binding site.

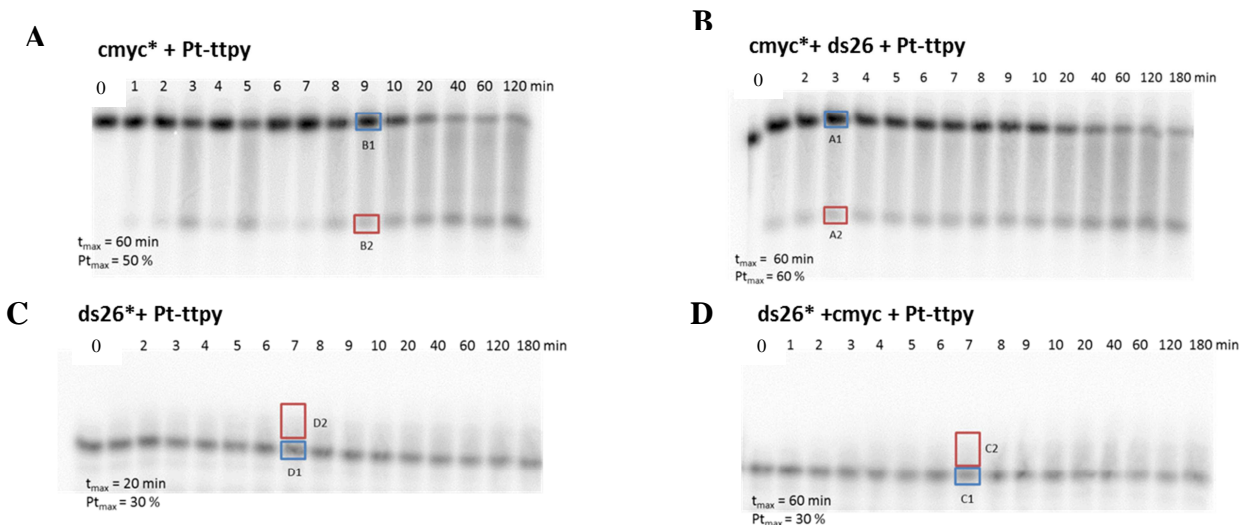


Figure S8. Kinetics of formation of platinated adduct of ^{32}P radiolabeled *c-myc** ($0.2 \mu\text{M}$) (A) and cold duplex DNA ds26 ($10 \mu\text{M}$) (B) or of ^{32}P radiolabeled ds26* ($10 \mu\text{M}$) (C) and cold *c-myc* ($0.2 \mu\text{M}$) (D) in the presence of **Pt-tt_{py}** ($5 \mu\text{M}$) in $\text{K}^+\text{10}$ buffer at 25°C followed by denaturing acrylamide gel electrophoresis.

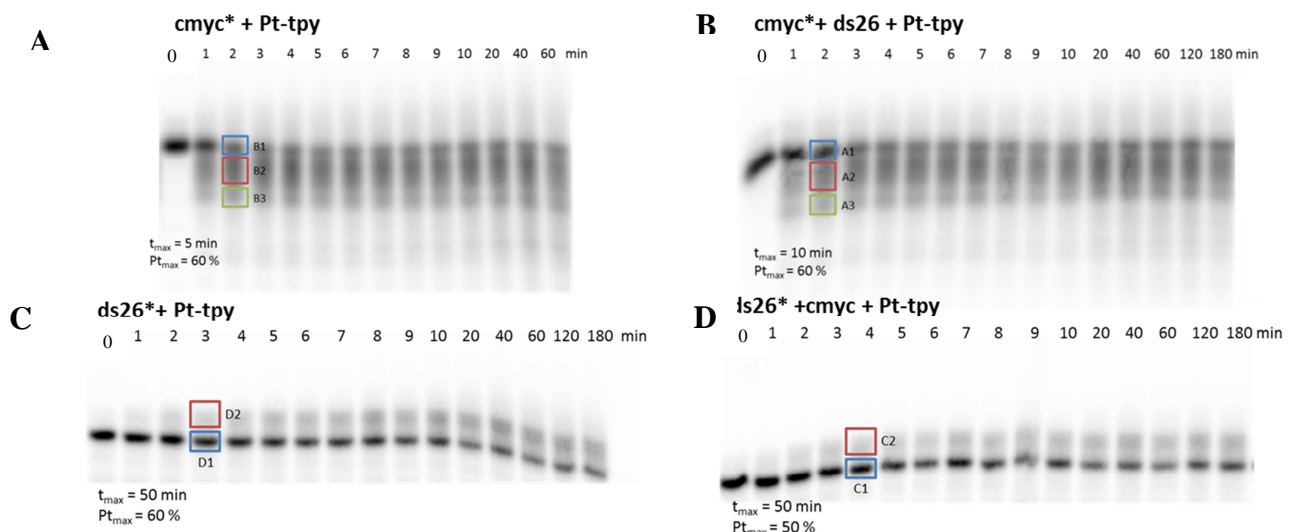


Figure S9. Kinetics of formation of platinated adduct of ^{32}P radiolabeled *c-myc** ($0.2 \mu\text{M}$) (A) and cold duplex DNA ds26 ($10 \mu\text{M}$) (B) or of ^{32}P radiolabeled ds26* ($10 \mu\text{M}$) (C) and cold *c-myc* ($0.2 \mu\text{M}$) (D) in the presence of **Pt-tt_{py}** ($5 \mu\text{M}$) in $\text{K}^+\text{10}$ buffer at 25°C followed by denaturing acrylamide gel electrophoresis.

Table S1: ΔT_m ($^{\circ}$ C) of F-21-T, F-c-myc-T, F-21CTA-T and F-CEB25-WT-T in the presence of **Pt-ctpy**, **Pt-BisQ**, **Pt-ttpp**, **Pt-tpy**, **Pt-vpym**, **Pt-cpym**, **Pt(PA)-tpy**, and PhenDC3.

Ligand	ΔT_m ($^{\circ}$ C)							
	F-21-T		F-c-myc-T		F-21CTA-T		F-CEB25-WT-T	
	0 μ M ds26	10 μ M ds26	0 μ M ds26	10 μ M ds26	0 μ M ds26	10 μ M ds26	0 μ M ds26	10 μ M ds26
Pt-ctpy	16.7 \pm 1.1	7.4 \pm 1.0	13.0 \pm 2.1	6.4 \pm 1.3	14.2 \pm 0.9	4.7 \pm 0.6	17.0 \pm 1.9	3.9 \pm 0.5
Pt-BisQ	20.6 \pm 2.0	8.9 \pm 1.0	10.3 \pm 1.8	3.7 \pm 0.4	10.6 \pm 1.3	0.4 \pm 0.5	15.6 \pm 4.1	3.9 \pm 0.6
Pt-ttpp	12.8 \pm 2.9	3.9 \pm 1.9	9.4 \pm 2.9	5.5 \pm 2.6	7.5 \pm 3.0	1.8 \pm 1.2	10.0 \pm 3.8	1.6 \pm 0.6
Pt-tpy	6.0 \pm 1.2	2.1 \pm 0.5	3.2 \pm 1.8	3.2 \pm 2.9	7.0 \pm 1.5	6.6 \pm 1.0	4.2 \pm 1.3	2.3 \pm 2.9
Pt-vpym	7.9 \pm 2.0	5.3 \pm 0.5	3.5 \pm 0.9	8.5 \pm 2.8	3.7 \pm 0.9	6.8 \pm 0.3	3.8 \pm 0.5	1.8 \pm 0.1
Pt-cpym	10.3 \pm 2.1	1.1 \pm 0.1	1.7 \pm 0.4	1.6 \pm 1.4	0.8 \pm 0.1	0.9 \pm 0.3	2.2 \pm 0.3	0.6 \pm 0.0
Pt(PA)-tpy	5.2 \pm 1.4	-1.0 \pm 0.4	0.4 \pm 0.5	0.4 \pm 0.7	0.3 \pm 0.3	-0.5 \pm 0.3	0.8 \pm 0.3	0.1 \pm 0.1
PhenDC3	24.3 \pm 1.4	24.4 \pm 1.0	21.3 \pm 1.2	21.7 \pm 0.7	18.4 \pm 1.0	14.6 \pm 1.2	22.0 \pm 1.3	19.8 \pm 1.7

Table S2: % of TO displacement at 1 μ M of ligand (**Pt-ctpy**, **Pt-BisQ**, **Pt-ttpp**, **Pt-tpy**, **Pt-cpym**, **Pt(PA)-tpy**, and PhenDC3) on 22AG, C-myc, 21CTA, CEB-25WT and ds26.

Ligand	% of TO displacement at 1 μ M of ligand				
	22AG	c-myc	21CTA	CEB25-WT	ds26
Pt-ctpy	88	76	93	82	17
Pt-BisQ	93	89	95	90	12
Pt-ttpp	80	64	87	66	nd
Pt-tpy	21	41	24	14	nd
Pt-cpym	67	33	82	43	2
Pt(PA)-tpy	55	59	52	37	nd
PhenDC3	95	96	95	90	nd

Table S3: % of TO-PRO-3 displacement at 1 μ M of ligand (**Pt-ctpy**, **Pt-BisQ**, **Pt-ttpp**, **Pt-tpy**, **Pt-vpym**, **Pt-cpym**, **Pt(PA)-tpy**, and PhenDC3) on 22AG, C-myc, 21CTA, CEB-25WT and ds26.

Ligand	% of TOPRO3 displacement at 1 μ M of ligand				
	22AG	c-myc	21CTA	CEB25-WT	ds26
Pt-ctpy	78	58	83	76	24
Pt-BisQ	62	44	57	69	5
Pt-ttpp	65	76	62	62	13
Pt-tpy	12	32	23	nd	nd
Pt-vpym	28	32	32	23	nd
Pt-cpym	25	nd	25	nd	nd
Pt(PA)-tpy	nd	nd	3	nd	nd
PhenDC3	85	73	83	88	nd

Table S4: % of PhenDV displacement at 1 μ M of ligand (**Pt-ctpy**, **Pt-BisQ**, **Pt-ttpy**, **Pt-tpy**, **Pt-cpym**, **Pt(PA)-tpy**, and PhenDC3) on 22AG, C-myc, 21CTA and CEB25-WT.

Ligand	% of PhenDV displacement at 1 μ M of ligand			
	22AG	c-myc	21CTA	CEB25-WT
Pt-ctpy	84	29	100	72
Pt-BisQ	64	20	94	45
Pt-ttpy	63	22	90	45
Pt-tpy	24	5	35	13
Pt-cpym	43	3	72	33
Pt(PA)-tpy	20	2	34	13
PhenDC3	92	85	100	99